

A PARALLEL ROBIN-ROBIN DOMAIN DECOMPOSITION METHOD FOR THE STOKES-DARCY SYSTEM*

WENBIN CHEN[†], MAX GUNZBURGER[‡], FEI HUA[§], AND XIAOMING WANG[¶]

Abstract. We propose a new parallel Robin-Robin domain decomposition method for the coupled Stokes-Darcy system with Beavers-Joseph-Saffman-Jones interface boundary condition. In particular, we prove that, with an appropriate choice of parameters, the scheme converges geometrically independent of the mesh size.

Key words. Stokes and Darcy equations, Robin-Robin domain decomposition, geometrical convergence

AMS subject classifications. 65N55, 65N30, 35M20, 35Q35

1. Introduction. The Darcy equations are a well accepted model for flow in porous media such as that that is often found in the subsurface. Thus, discretized versions of these equations are often used to simulate both groundwater and petroleum flows. However, in these settings, one often finds that what the porous media does not completely cover subsurface regions of interest. For examples, in petroleum applications, one often finds pockets of oil and in karst aquifers, one finds conduits in which free water flows. In such regions, the flow of the liquid cannot be accurately modeled by the Darcy equations, even though often, for expediency, that is exactly what is done in practice. A more accurate description of the flow of liquids in cavities and conduits is given by the Navier-Stokes equations. Due to the relative slow flows often encountered in such situations, one can simplify matters and use the linear Stokes equations instead. Of course, flows in conduits and cavities are coupled to the flow in the surrounding porous media so that conditions along the interfaces separating free flows and porous media flows must be imposed to effect the coupling. Several such interface conditions have been proposed; see, e.g., [1, 19]. Once a coupled Stokes-Darcy system has been defined, the remaining tasks are to define discrete systems whose solutions accurately approximate the exact solution of the continuous model and then to develop efficient methods for solving the discrete equations. These are the tasks that we address in this paper.

Here we consider a coupled Stokes-Darcy system on a bounded domain $\Omega = \Omega_p \cup \Omega_f \subset \mathbb{R}^d$, ($d = 2, 3$). In the porous media region Ω_p , the governing equations

*Supported in part by the SCRMS program of the National Science Foundation under grant number DMS-0724273.

[†]School of Mathematical Science, Fudan University, Shanghai, P.R.China, 200433, wchen@fudan.edu.cn. Supported by the Chinese MOE under an 111 project grant, the National Basic Research Program under grant number 2005CB321701, and the Shanghai Natural Science Foundation under grant number 07JC14001.

[‡]Department of Scientific Computing, Florida State University, Tallahassee FL 32306-4120, gunzburg@fsu.edu. Supported in part by the CMG program of the National Science Foundation under grant number DMS-0620035.

[§]Department of Mathematics, Florida State University, Tallahassee FL 32306-4120, fhua@math.fsu.edu. Supported in part by the CMG program of the National Science Foundation under grant number DMS-0620035.

[¶]Department of Mathematics, Florida State University, Tallahassee FL 32306-4120, wxm@math.fsu.edu. Supported in part by the CMG program of the National Science Foundation under grant number DMS-0620035.

are the Darcy equations

$$\begin{aligned}\mathbf{u}_p &= -\mathbb{K}\nabla\phi_p \\ \nabla \cdot \mathbf{u}_p &= 0,\end{aligned}$$

where \mathbf{u}_p is the fluid velocity in the porous media, \mathbb{K} is the hydraulic conductivity tensor, and ϕ_p is the hydraulic head. In the fluid region Ω_f , the fluid flow is assumed to satisfy the Stokes equations

$$\begin{aligned}-\nabla \cdot \mathbb{T}(\mathbf{u}_f, p_f) &= \mathbf{f} \\ \nabla \cdot \mathbf{u}_f &= 0,\end{aligned}$$

where \mathbf{u}_f is the fluid velocity, p_f is the kinematic pressure, \mathbf{f} is the external body force, ν the kinematic viscosity of the fluid, $\mathbb{T}(\mathbf{u}_f, p_f) = 2\nu\mathbb{D}(\mathbf{u}_f) - p_f\mathbb{I}$ is the stress tensor, and $\mathbb{D}(\mathbf{u}_f) = 1/2(\nabla\mathbf{u}_f + \nabla^T\mathbf{u}_f)$ is the deformation tensor.

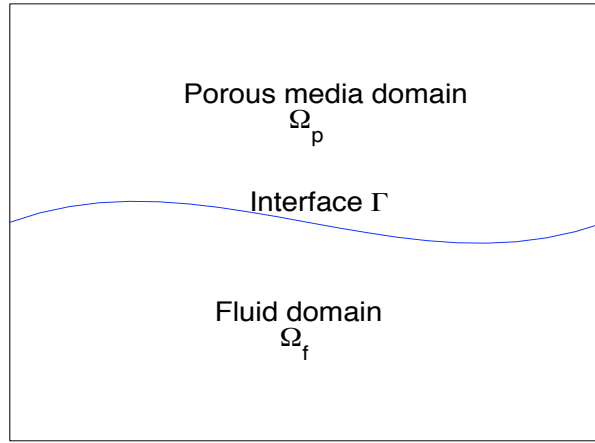


FIG. 1.1. The fluid and porous media domains Ω_f and Ω_p , respectively, and the interface Γ .

Let $\bar{\Gamma} = \bar{\Omega}_p \cap \bar{\Omega}_f$ denote the interface between the fluid and porous media regions; see Fig. 1.1. Along the interface Γ , we require

$$\mathbf{u}_f \cdot \mathbf{n}_f = -\mathbf{u}_p \cdot \mathbf{n}_p, \quad (1.1)$$

$$-\boldsymbol{\tau}_j \cdot (\mathbb{T}(\mathbf{u}_f, p_f) \cdot \mathbf{n}_f) = \alpha \boldsymbol{\tau}_j \cdot \mathbf{u}_f, \quad (1.2)$$

$$-\mathbf{n}_f \cdot (\mathbb{T}(\mathbf{u}_f, p_f) \cdot \mathbf{n}_f) = g\phi_p, \quad (1.3)$$

where \mathbf{n}_f and \mathbf{n}_p denote the unit outer normal to the fluid and the porous media regions at the interface Γ , respectively; $\boldsymbol{\tau}_j$ ($j = 1, \dots, d-1$) denote mutually orthogonal unit tangential vectors to the interface Γ ; and the constant parameter α depends on ν and \mathbb{K} . The second condition (1.2) is referred to as the Beavers-Joseph-Saffman-Jones (BJSJ) interface condition [12, 19] which is an approximation of the Beavers-Joseph interface boundary condition [1]. The BJSJ boundary condition is also related to the Navier's slip boundary condition.

To enable direct comparisons with the results of [8] and for simplicity, we assume that the hydraulic head ϕ_p and the fluid velocity \mathbf{u}_f satisfies homogeneous Dirichlet boundary condition except on Γ , i.e., $\phi_p = 0$ on the boundary $\partial\Omega_p \setminus \Gamma$ and $\mathbf{u}_f = 0$ on the boundary $\partial\Omega_f \setminus \Gamma$.

The spaces that we utilize are

$$\begin{aligned} X_f &= \{\mathbf{v}_f \in [H^1(\Omega_f)]^d \mid \mathbf{v}_f = 0 \text{ on } \partial\Omega_f \setminus \Gamma\} \\ Q_f &= L^2(\Omega_f) \\ X_p &= \{\psi_p \in H^1(\Omega_p) \mid \psi_p = 0 \text{ on } \partial\Omega_p \setminus \Gamma\}. \end{aligned}$$

For the domain D ($D = \Omega_f$ or Ω_p), $(\cdot, \cdot)_D$ denotes the L^2 inner product on the domain D , and $\langle \cdot, \cdot \rangle$ denotes the L^2 inner product on the interface Γ or the duality pairing between $H^{-1/2}(\Gamma)$ and $H_0^{1/2}(\Gamma)$.

With these notations, the weak formulation of the coupled Stokes-Darcy problem is given as follows [2, 8]: find $(\mathbf{u}_f, p_f) \in X_f \times Q_f$ and $\phi_p \in X_p$ such that

$$\begin{aligned} a_f(\mathbf{u}_f, \mathbf{v}_f) + b_f(\mathbf{v}_f, p_f) + ga_p(\phi_p, \psi_p) + \langle g\phi_p, \mathbf{v}_f \cdot \mathbf{n}_f \rangle - \langle g\mathbf{u}_f \cdot \mathbf{n}_f, \psi_p \rangle \\ + \alpha \langle P_\tau \mathbf{u}_f, P_\tau \mathbf{v}_f \rangle = (\mathbf{f}, \mathbf{v}_f)_{\Omega_f} \quad \forall \mathbf{v}_f \in X_f, \psi_p \in X_p, \end{aligned} \quad (1.4)$$

$$b_f(\mathbf{u}_f, q_f) = 0, \quad \forall q_f \in Q_f, \quad (1.5)$$

where the bilinear forms are defined as

$$\begin{aligned} a_p(\phi_p, \psi_p) &= (\mathbb{K} \nabla \phi_p, \nabla \psi_p)_{\Omega_p} \\ a_f(\mathbf{u}_f, \mathbf{v}_f) &= 2\nu (\mathbb{D}(\mathbf{u}_f), \mathbb{D}(\mathbf{v}_f))_{\Omega_f} \\ b_f(\mathbf{v}_f, q) &= -(\nabla \cdot \mathbf{v}_f, q)_{\Omega_f} \end{aligned}$$

and P_τ denoted the projection onto the tangent space on Γ , i.e.

$$P_\tau \mathbf{u} = \sum_{j=1}^{d-1} (\mathbf{u} \cdot \boldsymbol{\tau}_j) \boldsymbol{\tau}_j.$$

It is easy to see that the system (1.4) and (1.5) is well posed for $\mathbf{f} \in [L^2(\Omega_f)]^d$ [2, 8].

Since the governing equations are different for the fluid and the porous media region, it is natural to utilize a domain decomposition method so that off-the-shelf efficient solvers for the Darcy system and the Stokes system can be utilized [8]. The central issue is then to determine if the domain decomposition method convergence and its associated convergence rate. The main contribution of this paper is the development and analysis of a *new parallel domain decomposition method based on Robin boundary conditions that converges with a rate that, for appropriate choices of acceleration parameters, is independent of the mesh size*.

For classical second-order elliptic problems, a Robin-type domain decomposition method (DDM) was introduced in [13] where it was also proved that the solution of the Robin DDM converges weakly to the solution of the elliptic problems with respect to the H^1 norm. In [4, 5], new update techniques for the Robin data were introduced and it was proved that the weak convergence in H^1 could induce strong convergence. In [9], it was pointed out that a convergence rate $1 - O(h^{1/2})$ can be achieved in the case of two subdomains. Recently, a rigorous analysis for the case of many subdomains was given in [16, 17] where it was proved, in certain cases such as for a small number of subdomains, that the convergence rate could be $1 - O(h^{1/2} H^{-1/2})$, where H is the size

of the subdomain and h is the size of the finite element grid. In particular, the new term “winding number” was proposed in [17] to describe the depth of subdomains, and in the case of many subdomains and it was shown that the convergence rate not only depends on the mesh size h and the size H of subdomains, but also on the winding number. Furthermore, Robin-type DDMS for parabolic problems was also studied in [18].

In [8], two Robin DDMS for the Stokes-Darcy equations, one a serial version (sRR) and the other a parallel version (pRR), are considered and compared with the Dirichlet-Neumann DDMS [6, 7]; mesh-independent convergence rates were observed for serial Robin DDMS numerically but not proved rigorously. In addition to providing a rigorous analysis, in this paper, we treat the more general case of the Beavers-Joseph-Saffman-Jones interface boundary condition instead of the further simplified interface boundary conditions considered in [8]. However, the full Beavers-Joseph interface boundary condition is not treated here since well posedness in the steady state case is established only for particular choices of parameters [2]. Other algorithms that combine ideas from multi-grid and DDMS can be found in [14], where the authors proposed to solve the coupled problem directly on a coarse grid (with mesh size h_{coarse}) and then use the coarse solution to provide boundary conditions for the Stokes and Darcy systems at the interface so that they may be solved separately on a finer mesh (with mesh size of the order of $h_{coarse}^{\frac{3}{2}}$). For DDMS for other settings, and especially for the parallel Robin-Robin domain decomposition methods, one may refer to [4–8, 13, 15–17, 20, 21] and the references cited therein.

The rest of the paper is organized as follows. In Section 2, we propose the Robin boundary conditions at the interface for the Stokes and Darcy systems. A necessary and sufficient condition on the equivalence of the Stokes-Darcy system with Beavers-Joseph-Saffman-Jones interface boundary condition and the new decoupled Stokes and Darcy systems with Robin boundary conditions is derived. In Section 3, we propose our new parallel Robin-Robin domain decomposition method. We establish the convergence of the new scheme for the case of equal acceleration parameters $\gamma_f = \gamma_p$ and the case of $\gamma_f < \gamma_p$, with a convergence rate for appropriate choices of the acceleration parameters. Finite element approximations are considered in Section 4. In particular, we derive a convergence rate (depending on the mesh size h) for the case of equal acceleration parameters and the case of $\gamma_p < \gamma_f$. Although the convergence rate is derived for globally regular triangulations only, we may easily generalize the result to mortar elements so that solvers with different mesh size may be utilized for the fluid and the porous media regions. We present our results of some computational experiments in Section 5. These results are in accordance with our analyses.

2. Robin boundary conditions. In order to solve the coupled Stokes-Darcy problem utilizing the domain decomposition idea, we naturally consider (partial) Robin boundary conditions for the Stokes and the Darcy equations because Robin boundary conditions are more general and embody both the Neumann and Dirichlet type conditions in (1.1)–(1.3).

Let us consider the following Robin condition for the Darcy system: for a given constant $\gamma_p > 0$ and a given function η_p defined on Γ ,

$$\gamma_p \mathbb{K} \nabla \widehat{\phi}_p \cdot \mathbf{n}_p + g \widehat{\phi}_p = \eta_p \quad \text{on } \Gamma. \quad (2.1)$$

Then, the corresponding weak formulation for the Darcy system is given by: for

$\eta_p \in L^2(\Gamma)$, find $\widehat{\phi}_p \in X_p$ such that

$$\gamma_p a_p(\widehat{\phi}_p, \psi_p) + \langle g\widehat{\phi}_p, \psi_p \rangle = \langle \eta_p, \psi_p \rangle \quad \forall \psi_p \in X_p.$$

Similarly, we propose the following Robin type condition for the Stokes equations: for a given constant $\gamma_f > 0$ and a given function η_f defined on Γ ,

$$\mathbf{n}_f \cdot (\mathbb{T}(\widehat{\mathbf{u}}_f, \widehat{p}_f) \cdot \mathbf{n}_f) + \gamma_f \widehat{\mathbf{u}}_f \cdot \mathbf{n}_f = \eta_f \quad \text{on } \Gamma. \quad (2.2)$$

Then, the corresponding weak formulation for the Stokes system is given by: for $\eta_f \in L^2(\Gamma)$, find $\widehat{\mathbf{u}}_f \in X_f$ and $\widehat{p}_f \in Q_f$ such that

$$\begin{aligned} a_f(\widehat{\mathbf{u}}_f, \mathbf{v}_f) + b_f(\mathbf{v}_f, \widehat{p}_f) + \gamma_f \langle \widehat{\mathbf{u}}_f \cdot \mathbf{n}_f, \mathbf{v}_f \cdot \mathbf{n}_f \rangle \\ + \alpha \langle P_\tau \widehat{\mathbf{u}}_f, P_\tau \mathbf{v}_f \rangle = (\mathbf{f}, \mathbf{v}_f)_{\Omega_f} + \langle \eta_f, \mathbf{v}_f \cdot \mathbf{n}_f \rangle \quad \forall \mathbf{v}_f \in X_f \\ b_f(\widehat{\mathbf{u}}_f, q_f) = 0 \quad \forall q_f \in Q_f. \end{aligned} \quad (2.3)$$

We can combine the Stokes and Darcy systems with Robin boundary conditions into one system. Indeed, for any positive constant ω , it is easy to see that if $\eta_p \in L^2(\Gamma)$ and $\eta_f \in L^2(\Gamma)$ are given, then, there exists a unique solution $(\widehat{\phi}_p, \widehat{\mathbf{u}}_f, \widehat{p}_f) \in X_p \times X_f \times Q_f$ such that

$$\begin{aligned} a_f(\widehat{\mathbf{u}}_f, \mathbf{v}_f) + b_f(\mathbf{v}_f, \widehat{p}_f) + \omega \gamma_p a_p(\widehat{\phi}_p, \psi_p) + \omega \langle g\widehat{\phi}_p, \psi_p \rangle + \gamma_f \langle \widehat{\mathbf{u}}_f \cdot \mathbf{n}_f, \mathbf{v}_f \cdot \mathbf{n}_f \rangle \\ + \alpha \langle P_\tau \widehat{\mathbf{u}}_f, P_\tau \mathbf{v}_f \rangle = (\mathbf{f}, \mathbf{v}_f)_{\Omega_f} + \langle \eta_f, \mathbf{v}_f \cdot \mathbf{n}_f \rangle + \omega \langle \eta_p, \psi_p \rangle \quad \forall \psi_p \in X_p, \mathbf{v}_f \in X_f \\ b_f(\widehat{\mathbf{u}}_f, q_f) = 0 \quad \forall q_f \in Q_f. \end{aligned} \quad (2.4)$$

REMARK. 2.1. Note that the solution $(\widehat{\phi}_p, \widehat{\mathbf{u}}_f, \widehat{p}_f)$ is independent of the parameter ω .

Our next goal is to show that, for appropriate choices of γ_f , γ_p , η_f , and η_p , (smooth) solutions of the Stokes-Darcy system are equivalent to solutions of (2.4), and hence we may solve the latter system instead of the former.

LEMMA 2.2. *Let $(\phi_p, \mathbf{u}_f, p_f)$ be the solution of the coupled Stokes-Darcy system (1.4)–(1.5) and let $(\widehat{\phi}_p, \widehat{\mathbf{u}}_f, \widehat{p}_f)$ be the solution of the decoupled Stokes and Darcy system with Robin boundary conditions at the interface (2.4). Then, $(\widehat{\phi}_p, \widehat{\mathbf{u}}_f, \widehat{p}_f) = (\phi_p, \mathbf{u}_f, p_f)$ if and only if γ_f , γ_p , η_f , and η_p satisfy the following compatibility conditions:*

$$\eta_p = \gamma_p \widehat{\mathbf{u}}_f \cdot \mathbf{n}_f + g\widehat{\phi}_p \quad (2.5)$$

$$\eta_f = \gamma_f \widehat{\mathbf{u}}_f \cdot \mathbf{n}_f - g\widehat{\phi}_p. \quad (2.6)$$

Proof. For the necessity, we set $\psi_p = 0$ in the Stokes-Darcy system (1.4)–(1.5) and deduce that $(\phi_p, \mathbf{u}_f, p_f)$ solves (2.3) if

$$\langle \eta_f - \gamma_f \mathbf{u}_f \cdot \mathbf{n}_f + g\phi_p, \mathbf{v}_f \cdot \mathbf{n}_f \rangle = 0 \quad \forall \mathbf{v}_f \in X_f \quad (2.7)$$

which implies (2.6). The necessity of (2.5) can be derived in a similar fashion.

As for the sufficiency, by setting $\omega = g/\gamma_p$ in (2.4) and substituting the compatibility conditions (2.5)–(2.6), we easily see that $(\widehat{\phi}_p, \widehat{\mathbf{u}}_f, \widehat{p}_f)$ solves the coupled Stokes-Darcy system (1.4)–(1.5).

Since the solution to the Stokes-Darcy system is unique, we have $(\widehat{\phi}_p, \widehat{\mathbf{u}}_f, \widehat{p}_f) = (\phi_p, \mathbf{u}_f, p_f)$. \square

3. Robin-Robin domain decomposition methods.

3.1. The Robin-Robin domain decomposition algorithm. Now we propose the following parallel Robin-Robin domain decomposition method for solving the coupled Stokes-Darcy system.

1. Initial values of η_p^0 and η_f^0 are guessed. They may be taken to be zero.
2. For $k = 1, 2, \dots$, independently solve the Stokes and Darcy systems with Robin boundary conditions. More precisely, $\phi_p^k \in X_p$ is computed from

$$\gamma_p a_p(\phi_p^k, \psi_p) + \langle g\phi_p^k, \psi_p \rangle = \langle \eta_p^k, \psi_p \rangle \quad \forall \psi_p \in X_p; \quad (3.1)$$

and $\mathbf{u}_f^k \in X_f$ and $p_f^k \in Q_f$ are computed from

$$\begin{aligned} a_f(\mathbf{u}_f^k, \mathbf{v}_f) + b_f(\mathbf{v}_f, p_f^k) + \gamma_f \langle \mathbf{u}_f^k \cdot \mathbf{n}_f, \mathbf{v}_f \cdot \mathbf{n}_f \rangle + \alpha \langle P_\tau \mathbf{u}_f^k, P_\tau \mathbf{v}_f \rangle \\ = \langle \eta_f^k, \mathbf{v}_f \cdot \mathbf{n}_f \rangle + (\mathbf{f}, \mathbf{v}_f)_{\Omega_f} \quad \forall \mathbf{v}_f \in X_f, \end{aligned} \quad (3.2)$$

$$b_f(\mathbf{u}_f^k, q_f) = 0 \quad \forall q_f \in Q_f. \quad (3.3)$$

3. η_p^{k+1} and η_f^{k+1} are updated in the following manner:

$$\eta_f^{k+1} = a\eta_p^k + bg\phi_p^k \quad (3.4)$$

$$\eta_p^{k+1} = c\eta_f^k + d\mathbf{u}_f^k \cdot \mathbf{n}_f \quad (3.5)$$

where the coefficients a, b, c, d are chosen as follows:

$$a = \frac{\gamma_f}{\gamma_p} \quad b = -1 - a \quad (3.6)$$

$$c = -1 \quad d = \gamma_f + \gamma_p. \quad (3.7)$$

In the special case for which $\gamma_f = \gamma_p = \gamma$, we have

$$a = 1 \quad b = -2 \quad c = -1 \quad d = 2\gamma.$$

The relations (3.6)–(3.7) are necessary to ensure the convergence of the scheme. Indeed, suppose that η_f^k and η_p^k converge to η_f^* and η_p^* , respectively, and ϕ_p^k, \mathbf{u}_f^k also converge to the true solution ϕ_p^* and \mathbf{u}_f^* , respectively. Then, by (3.4)–(3.5) and Lemma 2.2, we see that the following relationships hold:

$$\eta_f^* = a\eta_p^* + bg\phi_p^* = \gamma_f \mathbf{u}_f^* \cdot \mathbf{n}_f - g\phi_p^*, \quad (3.8)$$

$$\eta_p^* = c\eta_f^* + d\mathbf{u}_f^* \cdot \mathbf{n}_f = \gamma_p \mathbf{u}_f^* \cdot \mathbf{n}_f + g\phi_p^*. \quad (3.9)$$

This leads to

$$\begin{aligned} \begin{pmatrix} bg\phi_p^* \\ d\mathbf{u}_f^* \cdot \mathbf{n}_f \end{pmatrix} &= \begin{pmatrix} b & 0 \\ 0 & d \end{pmatrix} \begin{pmatrix} g\phi_p^* \\ \mathbf{u}_f^* \cdot \mathbf{n}_f \end{pmatrix} = \begin{pmatrix} 1 & -a \\ -c & 1 \end{pmatrix} \begin{pmatrix} \eta_f^* \\ \eta_p^* \end{pmatrix} \\ &= \begin{pmatrix} 1 & -a \\ -c & 1 \end{pmatrix} \begin{pmatrix} -1 & \gamma_f \\ 1 & \gamma_p \end{pmatrix} \begin{pmatrix} g\phi_p^* \\ \mathbf{u}_f^* \cdot \mathbf{n}_f \end{pmatrix} \end{aligned} \quad (3.10)$$

which implies the consistency equations (3.6)–(3.7) on the coefficients a, b, c, d and γ_f, γ_p .

These relationships (3.6)–(3.7) among the parameters are used in the convergence analysis of the Robin-Robin domain decomposition method.

REMARK. 3.1. If the updating strategy (3.4)–(3.5) is changed to

$$\begin{aligned}\eta_f^{k+1} &= a_1\eta_p^k + b_1g\phi_p^k + c_1\mathbf{u}_f^k \cdot \mathbf{n}_f \\ \eta_p^{k+1} &= a_2\eta_f^k + b_2g\phi_p^k + c_2\mathbf{u}_f^k \cdot \mathbf{n}_f,\end{aligned}$$

then, the “consistency” conditions change to

$$\begin{pmatrix} -a_1 & 1 \\ 1 & a_2 \end{pmatrix} \begin{pmatrix} 1 & \gamma_p \\ -1 & \gamma_f \end{pmatrix} = \begin{pmatrix} b_1 & c_1 \\ b_2 & c_2 \end{pmatrix}.$$

In this case, we have more flexibility. However, the convergence analysis is somewhat more complicated, and will be addressed elsewhere.

The parallel Robin-Robin domain decomposition algorithm proposed here is related to the serial version (sRR algorithm) of [8]. As a matter of fact, the sRR algorithm can be obtained by implementing our algorithm serially as follows. Initialize η_p^0 , and, for $k = 0, 1, \dots$,

1. Find ϕ_p^k by solving the Darcy system (3.1).
2. Set $\eta_f^k = a\eta_p^k + bg\phi_p^k$ and find \mathbf{u}_f^k and p_f^k by solving the Stokes system (3.2)–(3.3).
3. Set $\eta_p^{k+1} = c\eta_f^k + d\mathbf{u}_f^k \cdot \mathbf{n}_f$.

In [8], it is proved, for $\gamma_f = \gamma_p = \gamma$, that the solution of the sRR algorithm converges to the solution of the Darcy-Stokes systems. Here, we are able to prove a similar convergence result. Moreover, we are able to demonstrate that the convergence could be geometric for appropriate choice of $\gamma_f < \gamma_p$.

3.2. Convergence of the parallel Robin-Robin DDM. We follow the elegant energy method proposed in [13] to demonstrate the convergence of the parallel Robin-Robin domain decomposition method for appropriate choice of parameters γ_p and γ_f .

To this end, let $(\phi_p, \mathbf{u}_f, p_f)$ denote the solution of the coupled Stokes-Darcy system (1.4)–(1.5). Then, we have that $(\phi_p, \mathbf{u}_f, p_f)$ solves the equivalent decoupled system (2.4) with $\gamma_f, \gamma_p, \eta_p, \eta_f$ satisfying the compatibility conditions (2.5)–(2.6) with the hats removed.

Next, we define the error functions

$$\begin{aligned}\epsilon_p^k &= \eta_p - \eta_p^k & \epsilon_f^k &= \eta_f - \eta_f^k \\ e_\phi^k &= \phi_p - \phi_p^k & \mathbf{e}_u^k &= \mathbf{u}_f - \mathbf{u}_f^k & e_p^k &= p_f - p_f^k.\end{aligned}$$

Then, the error functions satisfy the following error equations:

$$\gamma_p a_p(e_\phi^k, \psi_p) + \langle g e_\phi^k, \psi_p \rangle = \langle \epsilon_p^k, \psi_p \rangle \quad \forall \psi_p \in X_p, \quad (3.11)$$

$$\begin{aligned}a_f(\mathbf{e}_u^k, \mathbf{v}_f) + b_f(\mathbf{v}_f, e_p^k) + \gamma_f \langle \mathbf{e}_u^k \cdot \mathbf{n}_f, \mathbf{v}_f \cdot \mathbf{n}_f \rangle + \alpha \langle P_\tau \mathbf{e}_u^k, P_\tau \mathbf{v}_f \rangle \\ = \langle \epsilon_f^k, \mathbf{v}_f \cdot \mathbf{n}_f \rangle \quad \forall \mathbf{v}_f \in X_f,\end{aligned} \quad (3.12)$$

$$b_f(\mathbf{e}_u^k, q_f) = 0 \quad \forall q_f \in Q_f, \quad (3.13)$$

and, along the interface Γ ,

$$\epsilon_f^{k+1} = a\epsilon_p^k + bge_\phi^k \quad (3.14)$$

$$\epsilon_p^{k+1} = c\epsilon_f^k + d\mathbf{e}_u^k \cdot \mathbf{n}_f. \quad (3.15)$$

Equation (3.15) leads to

$$\|\epsilon_p^{k+1}\|_\Gamma^2 = c^2 \|\epsilon_f^k\|_\Gamma^2 + d^2 \|\mathbf{e}_u^k \cdot \mathbf{n}_f\|_\Gamma^2 + 2cd \langle \epsilon_f^k, \mathbf{e}_u^k \cdot \mathbf{n}_f \rangle.$$

Setting $\mathbf{v}_f = \mathbf{e}_u^k$ in (3.12), we deduce

$$\langle \epsilon_f^k, \mathbf{e}_u^k \cdot \mathbf{n}_f \rangle = a_f(\mathbf{e}_u^k, \mathbf{e}_u^k) + \gamma_f \|\mathbf{e}_u^k \cdot \mathbf{n}_f\|_\Gamma^2 + \alpha \|P_\tau \mathbf{e}_u^k\|_\Gamma^2$$

and, hence, combining the last two equations, we have

$$\|\epsilon_p^{k+1}\|_\Gamma^2 = c^2 \|\epsilon_f^k\|_\Gamma^2 + (d^2 + 2cd\gamma_f) \|\mathbf{e}_u^k \cdot \mathbf{n}_f\|_\Gamma^2 + 2cd a_f(\mathbf{e}_u^k, \mathbf{e}_u^k) + 2cd \alpha \|P_\tau \mathbf{e}_u^k\|_\Gamma^2. \quad (3.16)$$

Similarly, (3.14) implies

$$\|\epsilon_f^{k+1}\|_\Gamma^2 = a^2 \|\epsilon_p^k\|_\Gamma^2 + b^2 \|ge_\phi^k\|_\Gamma^2 + 2ab \langle \epsilon_p^k, ge_\phi^k \rangle.$$

Setting $\psi_p = ge_\phi^k$ in (3.11), we have

$$\langle \epsilon_p^k, ge_\phi^k \rangle = \gamma_p a_p(e_\phi^k, ge_\phi^k) + \langle ge_\phi^k, ge_\phi^k \rangle.$$

Combining the last two equations, we deduce

$$\|\epsilon_f^{k+1}\|_\Gamma^2 = a^2 \|\epsilon_p^k\|_\Gamma^2 + (b^2 + 2ab) \|ge_\phi^k\|_\Gamma^2 + 2ab\gamma_p g a_p(e_\phi^k, e_\phi^k). \quad (3.17)$$

Substituting (3.6)–(3.7) into (3.16) and (3.17), we have the following result.

LEMMA 3.2. *The error functions satisfy*

$$\begin{aligned} \|\epsilon_p^{k+1}\|_\Gamma^2 &= \|\epsilon_f^k\|_\Gamma^2 + (\gamma_p^2 - \gamma_f^2) \|\mathbf{e}_u^k \cdot \mathbf{n}_f\|_\Gamma^2 \\ &\quad - 2(\gamma_f + \gamma_p) a_f(\mathbf{e}_u^k, \mathbf{e}_u^k) - 2(\gamma_f + \gamma_p) \alpha \|P_\tau \mathbf{e}_u^k\|_\Gamma^2 \\ \|\epsilon_f^{k+1}\|_\Gamma^2 &= \left(\frac{\gamma_f}{\gamma_p} \right)^2 \|\epsilon_p^k\|_\Gamma^2 + \left(1 - \left(\frac{\gamma_f}{\gamma_p} \right)^2 \right) \|ge_\phi^k\|_\Gamma^2 - 2\gamma_f \left(1 + \frac{\gamma_f}{\gamma_p} \right) g a_p(e_\phi^k, e_\phi^k). \quad \blacksquare \end{aligned}$$

We are now ready to demonstrate the convergence of our parallel Robin-Robin domain decomposition method. The convergence analysis for $\gamma_f = \gamma_p$ and $\gamma_f \neq \gamma_p$ are different and will be treated separately.

Case 1: $\gamma_f = \gamma_p = \gamma$. In this case, we have

$$\begin{aligned} \|\epsilon_p^{k+1}\|_\Gamma^2 &= \|\epsilon_f^k\|_\Gamma^2 - 4\gamma a_f(\mathbf{e}_u^k, \mathbf{e}_u^k) - 4\gamma \alpha \|P_\tau \mathbf{e}_u^k\|_\Gamma^2 \\ \|\epsilon_f^{k+1}\|_\Gamma^2 &= \|\epsilon_p^k\|_\Gamma^2 - 4\gamma g a_p(e_\phi^k, e_\phi^k). \end{aligned}$$

Adding the two equations and summing over k from $k = 0$ to N , we deduce

$$\|\epsilon_p^{N+1}\|_\Gamma^2 + \|\epsilon_f^{N+1}\|_\Gamma^2 = \|\epsilon_p^0\|_\Gamma^2 + \|\epsilon_f^0\|_\Gamma^2 - 4\gamma \sum_{k=0}^N (a_f(\mathbf{e}_u^k, \mathbf{e}_u^k) + g a_p(e_\phi^k, e_\phi^k) + \alpha \|P_\tau \mathbf{e}_u^k\|_\Gamma^2).$$

This implies that $\|\epsilon_p^{N+1}\|_\Gamma^2 + \|\epsilon_f^{N+1}\|_\Gamma^2$ is bounded from above by $\|\epsilon_p^0\|_\Gamma^2 + \|\epsilon_f^0\|_\Gamma^2$ and that \mathbf{e}_u^k and e_ϕ^k tend to zero in $(H^1(\Omega_f))^d$ and $H^1(\Omega_p)$, respectively. The convergence of e_ϕ^k together with the error equation (3.11) implies the convergence of ϵ_p^k in $H^{-\frac{1}{2}}(\Gamma)$. Combining the convergence of ϵ_p^k and e_ϕ^k and the error equation on the interface (3.14), we deduce the convergence of ϵ_f^k in $H^{-\frac{1}{2}}(\Gamma)$. The convergence of the pressure then

follows from the inf-sup condition and (3.12)–(3.13). Note that we have no rate of convergence here. Hence, we have proved the following result.

THEOREM 3.3. *If $\gamma_p = \gamma_f = \gamma$, then*

$$\phi_p^k \xrightarrow{X_p} \phi_p \quad \mathbf{u}_f^k \xrightarrow{X_f} \mathbf{u}_f \quad p_f^k \xrightarrow{Q_f} p_f,$$

and

$$\eta_p^k \xrightarrow{H^{-\frac{1}{2}}(\Gamma)} \gamma \mathbf{u}_f \cdot \mathbf{n}_f + g\phi_p = -\gamma \mathbb{K} \nabla \phi_p \cdot \mathbf{n}_p + g\phi_p$$

$$\eta_f^k \xrightarrow{H^{-\frac{1}{2}}(\Gamma)} \gamma \mathbf{u}_f \cdot \mathbf{n}_f - g\phi_p = \mathbf{n}_f \cdot (\mathbb{T}(\mathbf{u}_f, p_f) \cdot \mathbf{n}_f) + \gamma \mathbf{u}_f \cdot \mathbf{n}_f. \quad \blacksquare$$

Case 2: $\gamma_f < \gamma_p$. In this case, because $e_\phi^k \in X_p$, we deduce that, thanks to the trace theorem and the Poincaré inequality, there exists a constant C_p (independent of \mathbb{K}) such that

$$\|e_\phi^k\|_\Gamma^2 \leq C_p \|\mathbb{K}^{-1}\| a_p(e_\phi^k, e_\phi^k). \quad (3.18)$$

Thus, if $\gamma_f < \gamma_p$ and

$$\frac{1}{\gamma_f} - \frac{1}{\gamma_p} \leq \frac{2}{gC_p \|\mathbb{K}^{-1}\|}, \quad (3.19)$$

we have

$$\begin{aligned} & \left(1 - \left(\frac{\gamma_f}{\gamma_p}\right)^2\right) \|ge_\phi^k\|_\Gamma^2 - 2\gamma_f \left(1 + \frac{\gamma_f}{\gamma_p}\right) ga_p(e_\phi^k, e_\phi^k) \\ & \leq \gamma_f g \left(1 + \frac{\gamma_f}{\gamma_p}\right) \left(\left(\frac{1}{\gamma_f} - \frac{1}{\gamma_p}\right) gC_p \|\mathbb{K}^{-1}\| - 2\right) a_p(e_\phi^k, e_\phi^k) \\ & \leq 0. \end{aligned}$$

Similarly, thanks to the trace theorem and Korn's inequality, there exists a constant C_f such that

$$\|\mathbf{e}_u^k \cdot \mathbf{n}_f\|_\Gamma^2 \leq C_f \int_{\Omega_f} |\mathbb{D}(\mathbf{e}_u^k)|^2 d\mathbf{x}.$$

Therefore, under the additional constraint

$$\gamma_p - \gamma_f \leq \frac{4\nu}{C_f},$$

we have

$$(\gamma_p^2 - \gamma_f^2) \|\mathbf{e}_u^k \cdot \mathbf{n}_f\|_\Gamma^2 \leq 2(\gamma_f + \gamma_p) a_f(\mathbf{e}_u^k, \mathbf{e}_u^k). \quad (3.20)$$

Hence we have, when combined with Lemma 3.2,

$$\|\epsilon_p^{k+1}\|_\Gamma^2 \leq \|\epsilon_f^k\|_\Gamma^2, \quad \|\epsilon_f^{k+1}\|_\Gamma^2 \leq \left(\frac{\gamma_f}{\gamma_p}\right)^2 \|\epsilon_p^k\|_\Gamma^2$$

which leads to

$$\|\epsilon_p^{k+1}\|_\Gamma \leq \frac{\gamma_f}{\gamma_p} \|\epsilon_p^{k-1}\|_\Gamma, \quad \|\epsilon_f^{k+1}\|_\Gamma \leq \frac{\gamma_f}{\gamma_p} \|\epsilon_f^{k-1}\|_\Gamma.$$

This implies the convergence of the η which further implies the convergence of the velocity \mathbf{e}_u^k , the pressure e_p^k , and the hydraulic head e_ϕ^k through the error equations (3.11) and (3.12)–(3.13).

Hence we have derived the following geometric convergence result.

THEOREM 3.4. *Assume that the parameters γ_p and γ_f are chosen so that*

$$0 < \gamma_p - \gamma_f \leq \frac{4\nu}{C_f} \quad \frac{1}{\gamma_f} - \frac{1}{\gamma_p} \leq \frac{2}{gC_p\|\mathbb{K}^{-1}\|}. \quad (3.21)$$

Then, the solutions of the parallel Robin-Robin domain decomposition method converge to the solution of the Stokes-Darcy system. Moreover,

$$a_p(e_\phi^k, e_\phi^k) + a_f(\mathbf{e}_u^k, \mathbf{e}_u^k) + \|e_p^k\|_\Gamma^2 + \|\epsilon_p^k\|_\Gamma^2 + \|\epsilon_f^k\|_\Gamma^2 \leq C \left(\frac{\gamma_f}{\gamma_p} \right)^{\lfloor \frac{k}{2} \rfloor} (\|e_p^0\|_\Gamma^2 + \|\epsilon_f^0\|_\Gamma^2).$$

The last inequality follows from the geometric convergence of $\epsilon_p^k, \epsilon_f^k$, the error relationship at the interface and the error equations.

4. Finite element approximations. We next consider finite element discretization of the Robin domain decomposition method that was proposed in the previous section. One of the advantages of considering finite element approximations is that we can then derive explicit convergence rates, even for the case $\gamma_f = \gamma_p = \gamma$. Of course, the rate of convergence will depend on the size of the element h . This is different from the case of $\gamma_f < \gamma_p$ where the rate of convergence is independent of h . We will also demonstrate the convergence of the finite element approximation even in the parameter region of $\gamma_p < \gamma_f$ which may seem unlikely in view of Lemma 3.2. One of the key advantages of the finite element setting is the availability of an inverse Poincaré type inequality [3] that allows us to control various terms.

We consider a regular triangulation \mathcal{T}_h of the global domain $\overline{\Omega}_p \cup \overline{\Omega}_f$ which is assumed to be regular and quasi-uniform. We also assume that the triangulation $\mathcal{T}_{f,h}, \mathcal{T}_{p,h}$ induced on the subdomains Ω_f and Ω_p are compatible on Γ and the mesh on the interface Γ is quasi-uniform. The induced triangulation on Γ will be denoted \mathcal{B}_h . Non-matching grid or mortar cases will be considered elsewhere. We denote by $X_{p,h} \subset X_p$ a finite element space on the porous media domain Ω_p and denote by $X_{f,h} \subset X_f$ and $Q_{f,h} \subset Q_f$ finite element spaces on the fluid domain Ω_f . We use these spaces to approximate the hydraulic head in the porous media and the fluid velocity and pressure.

Specifically, we choose

$$\begin{aligned} X_{p,h} &= \{ \psi_{p,h} \in C^0(\overline{\Omega}_p) \mid \psi_{p,h}|_T \in \mathbb{P}_2(T), \forall T \in \mathcal{T}_{p,h}, \psi_{p,h}|_{\partial\Omega_p \setminus \Gamma} = 0 \} \\ X_{f,h} &= \{ \mathbf{v}_{f,h} \in (C^0(\overline{\Omega}_f))^d \mid \mathbf{v}_{f,h}|_T \in (\mathbb{P}_2(T))^d, \forall T \in \mathcal{T}_{f,h}, \mathbf{v}_{f,h}|_{\partial\Omega_f \setminus \Gamma} = 0 \} \\ Q_{f,h} &= \{ q_{p,h} \in C^0(\overline{\Omega}_f) \mid q_{f,h}|_T \in \mathbb{P}_1(T), \forall T \in \mathcal{T}_{f,h} \}. \end{aligned}$$

The spaces $X_{f,h}$ and $Q_{f,h}$ are assumed to satisfy the discrete LBB or inf-sup condition [10, 11].

We also define the discrete trace space on the interface

$$Z_h = \{\eta_h \in C^0(\Gamma) \mid \eta_h|_\tau \in \mathbb{P}_2(\tau), \forall \tau \in \mathcal{B}_h, \eta_h|_{\partial\Gamma} = 0\}.$$

It is easy to see that Z_h is the trace space in the sense that

$$\begin{aligned} Y_{p,h} &:= X_{p,h}|_\Gamma = Z_h, \\ Y_{f,h} &:= X_{f,h}|_\Gamma \cdot \mathbf{n}_f = Z_h. \end{aligned}$$

The discrete weak formulation of the coupled Stokes-Darcy problem is then given by: find $(\mathbf{u}_{f,h}, p_{f,h}) \in X_{f,h} \times Q_{f,h}$ and $\phi_{p,h} \in X_{p,h}$ such that

$$\begin{aligned} a_f(\mathbf{u}_{f,h}, \mathbf{v}_f) + b_f(\mathbf{v}_f, p_{f,h}) + g a_p(\phi_{p,h}, \psi_p) + \langle g \phi_{p,h}, \mathbf{v}_f \cdot \mathbf{n}_f \rangle - \langle g \mathbf{u}_{f,h} \cdot \mathbf{n}_f, \psi_p \rangle \\ + \alpha \langle P_\tau \mathbf{u}_{f,h}, P_\tau \mathbf{v}_f \rangle = (\mathbf{f}, \mathbf{v}_f)_{\Omega_f} \quad \forall \mathbf{v}_f \in X_{f,h}, \psi_p \in X_{p,h} \\ b_f(\mathbf{u}_{f,h}, q_f) = 0, \quad \forall q_f \in Q_{f,h}. \end{aligned} \quad (4.1)$$

The FEM approximation of the decoupled Stokes-Darcy system with Robin boundary conditions (2.1)–(2.2) can be formulated in the following way: for given $\eta_{p,h} \in L^2(\Gamma)$ and $\eta_{f,h} \in L^2(\Gamma)$, find $(\widehat{\phi}_{p,h}, \widehat{\mathbf{u}}_{f,h}, \widehat{p}_{f,h}) \in X_{p,h} \times X_{f,h} \times Q_{f,h}$ such that

$$\begin{aligned} a_f(\widehat{\mathbf{u}}_{f,h}, \mathbf{v}_f) + b_f(\mathbf{v}_f, \widehat{p}_{f,h}) + \omega \gamma_p a_p(\widehat{\phi}_{p,h}, \psi_p) + \omega \langle g \widehat{\phi}_{p,h}, \psi_p \rangle + \gamma_f \langle \widehat{\mathbf{u}}_{f,h} \cdot \mathbf{n}_f, \mathbf{v}_f \cdot \mathbf{n}_f \rangle \\ + \alpha \langle P_\tau \widehat{\mathbf{u}}_{f,h}, P_\tau \mathbf{v}_f \rangle = (\mathbf{f}, \mathbf{v}_f)_{\Omega_f} + \langle \eta_{f,h}, \mathbf{v}_f \cdot \mathbf{n}_f \rangle + \omega \langle \eta_{p,h}, \psi_p \rangle, \quad \forall \psi_p \in X_{p,h}, \mathbf{v}_f \in X_{f,h} \\ b_f(\widehat{\mathbf{u}}_{f,h}, q_f) = 0, \quad \forall q_f \in Q_{f,h}. \end{aligned} \quad (4.2)$$

Similar to the continuous case, finite element approximations of the coupled Stokes-Darcy system, defined by (4.1), and of the revised Robin approximation, defined by (4.2), are related in the following fashion:

LEMMA 4.1. *For $\eta_{p,h} \in Y_{p,h}$ and $\eta_f \in Y_{f,h}$, $(\widehat{\phi}_{p,h}, \widehat{\mathbf{u}}_{f,h}, \widehat{p}_{f,h}) = (\phi_{p,h}, \mathbf{u}_{f,h}, p_{f,h})$ if and only if $\eta_{p,h}$ and $\eta_{f,h}$ satisfy*

$$\eta_{p,h} = P_{p,h}(\gamma_p \mathbf{u}_{f,h} \cdot \mathbf{n}_f + g \phi_{p,h}) \quad \eta_{f,h} = P_{f,h}(\gamma_f \mathbf{u}_{f,h} \cdot \mathbf{n}_f - g \phi_{p,h}),$$

where $P_{p,h}$ and $P_{f,h}$ are $L^2(\Gamma)$ -projections onto the spaces $Y_{p,h}$ and $Y_{f,h}$ respectively, i.e., for $v \in L^2(\Gamma)$,

$$\langle P_{p,h} v, w_p \rangle = \langle v, w_p \rangle \quad \forall w_p \in Y_{p,h} \quad \langle P_{f,h} v, w_f \rangle = \langle v, w_f \rangle \quad \forall w_f \in Y_{f,h}. \quad \blacksquare$$

REMARK. 4.2. Comparing with the Robin conditions (2.1) and (2.2), we see that we have heuristically used

$$\begin{aligned} P_{p,h}(\gamma_p \mathbb{K} \nabla \phi_{p,h} \cdot \mathbf{n}_p + g \phi_{p,h}) &= \eta_{p,h} \\ P_{f,h}(\mathbf{n}_f \cdot (T(\mathbf{u}_{f,h}, p_{f,h}) \cdot \mathbf{n}_f) + \gamma_f \mathbf{u}_{f,h} \cdot \mathbf{n}_f) &= \eta_{f,h}. \end{aligned}$$

The choices of the spaces $Y_{p,h}$ and $Y_{f,h}$ are not unique; other choices are also possible.

The parallel Robin-Robin domain decomposition finite element method is defined as follows.

1. The initial values of $\eta_{p,h}^0 \in Y_{p,h}$ and $\eta_{f,h}^0 \in Y_{f,h}$ are guessed; they may be taken to be zero.

2. For $k = 1, 2, \dots$, solve the discrete Stokes and Darcy systems with Robin conditions independently, i.e., $\phi_{p,h}^k \in X_{p,h}$ is determined from

$$\gamma_p a_p(\phi_{p,h}^k, \psi_p) + \langle g \phi_{p,h}^k, \psi_p \rangle = \langle \eta_{p,h}^k, \psi_p \rangle \quad \forall \psi_p \in X_{p,h};$$

and $\mathbf{u}_{f,h}^k \in X_{f,h}$ and $p_{f,h}^k \in Q_{f,h}$ are determined from

$$\begin{aligned} a_f(\mathbf{u}_{f,h}^k, \mathbf{v}_f) + b_f(\mathbf{v}_f, p_{f,h}^k) + \gamma_f \langle \mathbf{u}_{f,h}^k \cdot \mathbf{n}_f, \mathbf{v}_f \cdot \mathbf{n}_f \rangle + \alpha \langle P_\tau \mathbf{u}_{f,h}^k, P_\tau \mathbf{v}_f \rangle \\ = \langle \eta_{f,h}^k, \mathbf{v}_f \cdot \mathbf{n}_f \rangle + (\mathbf{f}, \mathbf{v}_f)_{\Omega_f} \quad \forall \mathbf{v}_f \in X_{f,h} \end{aligned}$$

$$b_f(\mathbf{u}_{f,h}^k, q_f) = 0 \quad \forall q_f \in Q_{f,h}.$$

3. $\eta_{p,h}^{k+1}$ and $\eta_{f,h}^{k+1}$ are updated by

$$\eta_{p,h}^{k+1} = P_{f,h}(a \eta_{p,h}^k + b g \phi_{p,h}^k) \quad \eta_{p,h}^{k+1} = P_{p,h}(c \eta_{f,h}^k + d \mathbf{u}_f^k \cdot \mathbf{n}_f).$$

One important observation is that $\eta_{p,h}^k, \eta_{f,h}^k, \phi_{p,h}^k|_\Gamma, \mathbf{u}_f^k \cdot \mathbf{n}_f|_\Gamma \in Z_h$ for all k , provided that the initial guesses belong to Z_h . Therefore, the projections $P_{p,h}$ and $P_{f,h}$ in the implementation of the algorithm are identity operators.

We now consider the error functions for finite element approximations, just as in the continuous case studied in the previous section. Let

$$\begin{aligned} \epsilon_{p,h}^k &= \eta_{p,h} - \eta_{p,h}^k & \epsilon_{f,h}^k &= \eta_{f,h} - \eta_{f,h}^k, \\ e_{\phi,h}^k &= \phi_{p,h} - \phi_{p,h}^k & \mathbf{e}_{u,h}^k &= \mathbf{u}_{f,h} - \mathbf{u}_{f,h}^k & e_{p,h}^k &= p_{f,h} - p_{f,h}^k. \end{aligned}$$

It is straightforward to verify that

$$\epsilon_{p,h}^k \in Z_h \quad \epsilon_{f,h}^k \in Z_h \quad e_{\phi,h}^k|_\Gamma \in Z_h \quad \mathbf{e}_{u,h}^k \cdot \mathbf{n}_f \in Z_h.$$

It is also easy to see that the error functions satisfy the error equations

$$\gamma_p a_p(e_{\phi,h}^k, \psi_p) + \langle g e_{\phi,h}^k, \psi_p \rangle = \langle \epsilon_{p,h}^k, \psi_p \rangle \quad \forall \psi_p \in X_{p,h}, \quad (4.3)$$

$$\begin{aligned} a_f(\mathbf{e}_{u,h}^k, \mathbf{v}_f) + b_f(\mathbf{v}_f, e_{p,h}^k) + \gamma_f \langle \mathbf{e}_{u,h}^k \cdot \mathbf{n}_f, \mathbf{v}_f \cdot \mathbf{n}_f \rangle + \alpha \langle P_\tau \mathbf{e}_{f,h}^k, P_\tau \mathbf{v}_f \rangle \\ = \langle \epsilon_{f,h}^k, \mathbf{v}_f \cdot \mathbf{n}_f \rangle \quad \forall \mathbf{v}_f \in X_{f,h} \end{aligned} \quad (4.4)$$

$$b_f(\mathbf{e}_{u,h}^k, q_f) = 0 \quad \forall q_f \in Q_{f,h}, \quad (4.5)$$

and, along the interface,

$$\epsilon_{f,h}^{k+1} = P_{f,h}(a \epsilon_{p,h}^k + b g e_{\phi,h}^k) \quad \epsilon_{p,h}^{k+1} = P_{p,h}(c \epsilon_{f,h}^k + d \mathbf{e}_{u,h}^k \cdot \mathbf{n}_f).$$

It is easy to verify the following relationship for the error functions, just as in the continuous case.

LEMMA 4.3. *The error functions satisfy*

$$\begin{aligned} \|\epsilon_{p,h}^{k+1}\|_\Gamma^2 &= \|\epsilon_{f,h}^k\|_\Gamma^2 + (\gamma_p^2 - \gamma_f^2) \|\mathbf{e}_{u,h}^k \cdot \mathbf{n}\|_\Gamma^2 - 2(\gamma_f + \gamma_p) a_f(\mathbf{e}_{u,h}^k, \mathbf{e}_{u,h}^k) - 2(\gamma_f + \gamma_p) \|P_\tau \mathbf{e}_{u,h}^k\|_\Gamma^2 \\ \|\epsilon_{f,h}^{k+1}\|_\Gamma^2 &= \left(\frac{\gamma_f}{\gamma_p} \right)^2 \|\epsilon_{p,h}^k\|_\Gamma^2 + \left(1 - \left(\frac{\gamma_f}{\gamma_p} \right)^2 \right) \|g e_{\phi,h}^k\|_\Gamma^2 - 2\gamma_f \left(1 + \frac{\gamma_f}{\gamma_p} \right) g a_p(e_{\phi,h}^k, e_{\phi,h}^k). \quad \blacksquare \end{aligned}$$

The key ingredient in deriving an explicit convergence rate for the case of $\gamma_f = \gamma_p$ is the following estimate.

LEMMA 4.4.

$$\|\epsilon_{p,h}^k\|_{\Gamma}^2 \leq C(\|\mathbb{K}^{-1}\|^{1/2} + \gamma_p h^{-1/2} \|\mathbb{K}\|^{1/2})^2 a_p(e_{\phi,h}^k, e_{\phi,h}^k).$$

Proof. The key in the proof of this lemma is an extension operator. Let $\mathcal{N}_{p,h}$ be the set of nodes for the finite element triangulation on $\overline{\Omega}_p$, and let $\mathcal{N}_{p,\Gamma} = \mathcal{N}_{p,h}|_{\Gamma}$. Denote $E_{p,h}$ the zero extension operator from $Y_{p,h} = Z_h$ to $X_{p,h}$:

$$E_{p,h}\epsilon_{p,h}^k(P) = \begin{cases} \epsilon_{p,h}^k(P) & \text{if } P \in \mathcal{N}_{p,\Gamma} \\ 0 & \text{if } P \in \mathcal{N}_{p,h} \setminus \mathcal{N}_{p,\Gamma}. \end{cases}$$

Then, we have

$$\|E_{p,h}\epsilon_{p,h}^k\|_{L^2(\Omega_p)}^2 \approx h^d \sum_{P \in \mathcal{N}_{p,h}} (E_{p,h}\epsilon_{p,h}^k(P))^2 \approx h^d \sum_{P \in \mathcal{N}_{p,\Gamma}} (\epsilon_{p,h}^k(P))^2 \approx h \|\epsilon_{p,h}^k\|_{\Gamma}^2. \quad (4.6)$$

Note that $E_{p,h}\epsilon_{p,h}^k \in X_{p,h}$ due to the definition of the extension operator and the fact that $\epsilon_{p,h}^k \in Z_h$. Hence, we may set $\psi_p = E_{p,h}\epsilon_{p,h}^k$ in (4.3) and utilize Cauchy-Schwarz inequality to deduce

$$\begin{aligned} \|\epsilon_{p,h}^k\|_{\Gamma}^2 &= \gamma_p a_p(e_{\phi,h}^k, E_{p,h}\epsilon_{p,h}^k) + \langle g e_{\phi,h}^k, \epsilon_{p,h}^k \rangle \\ &\leq \gamma_p a_p(e_{\phi,h}^k, e_{\phi,h}^k)^{1/2} a_p(E_{p,h}\epsilon_{p,h}^k, E_{p,h}\epsilon_{p,h}^k)^{1/2} + \|g e_{\phi,h}^k\|_{\Gamma} \|\epsilon_{p,h}^k\|_{\Gamma}. \end{aligned} \quad (4.7)$$

On the other hand, thanks to the inverse inequality for finite element spaces and (4.6), we deduce

$$\begin{aligned} a_p(E_{p,h}\epsilon_{p,h}^k, E_{p,h}\epsilon_{p,h}^k) &\leq \|\mathbb{K}\| \|\nabla E_{p,h}\epsilon_{p,h}^k\|_{L^2(\Omega_p)}^2 \\ &\leq C h^{-2} \|\mathbb{K}\| \|E_{p,h}\epsilon_{p,h}^k\|_{L^2(\Omega_p)}^2 \leq C h^{-1} \|\mathbb{K}\| \|\epsilon_{p,h}^k\|_{\Gamma}^2. \end{aligned} \quad (4.8)$$

Combining the inequality (3.18) with (4.7)–(4.8), we obtain

$$\|\epsilon_{p,h}^k\|_{\Gamma}^2 \leq C \gamma_p h^{-1/2} \|\mathbb{K}\|^{1/2} a_p(e_{\phi,h}^k, e_{\phi,h}^k)^{1/2} \|\epsilon_{p,h}^k\|_{\Gamma} + C_p^{1/2} \|\mathbb{K}^{-1}\|^{1/2} a_p(e_{\phi,h}^k, e_{\phi,h}^k)^{1/2} \|\epsilon_{p,h}^k\|_{\Gamma}$$

which implies the lemma. \square

REMARK. 4.5. Similar results are available for P_1 conforming and nonconforming elements for classical second-order elliptic problems ([16, 17]).

Now for $\gamma_f = \gamma_p = \gamma$, by Lemma 4.3, we have

$$\begin{aligned} \|\epsilon_{p,h}^{k+1}\|_{\Gamma}^2 &= \|\epsilon_{f,h}^k\|_{\Gamma}^2 - 4\gamma a_f(\mathbf{e}_{u,h}^k, \mathbf{e}_{u,h}^k) - 4\gamma \|P_{\tau} \mathbf{e}_{u,h}^k\|_{\Gamma}^2 \\ \|\epsilon_{f,h}^{k+1}\|_{\Gamma}^2 &= \|\epsilon_{p,h}^k\|_{\Gamma}^2 - 4\gamma g a_p(e_{\phi,h}^k, e_{\phi,h}^k). \end{aligned}$$

Combining the above equalities with Lemma 4.4, we deduce

$$\|\epsilon_{p,h}^{k+1}\|_{\Gamma}^2 \leq \|\epsilon_{f,h}^k\|_{\Gamma}^2, \quad \|\epsilon_{f,h}^{k+1}\|_{\Gamma}^2 \leq (1 - C\gamma(\|\mathbb{K}^{-1}\|^{1/2} + \gamma h^{-\frac{1}{2}} \|\mathbb{K}\|^{1/2})^{-2}) \|\epsilon_{p,h}^k\|_{\Gamma}^2.$$

Therefore, we have proved the following lemma.

LEMMA 4.6. *For $\gamma_f = \gamma_p = \gamma$, we have*

$$\begin{aligned} \|\epsilon_{p,h}^{k+1}\|_{\Gamma}^2 &\leq (1 - C\gamma(\|\mathbb{K}^{-1}\|^{1/2} + \gamma h^{-1/2} \|\mathbb{K}\|^{1/2})^{-2}) \|\epsilon_{p,h}^{k-1}\|_{\Gamma}^2 \\ \|\epsilon_{f,h}^{k+1}\|_{\Gamma}^2 &\leq (1 - C\gamma(\|\mathbb{K}^{-1}\|^{1/2} + \gamma h^{-1/2} \|\mathbb{K}\|^{1/2})^{-2}) \|\epsilon_{f,h}^{k-1}\|_{\Gamma}^2. \quad \blacksquare \end{aligned}$$

This further implies convergence with convergence rate proportional to $1 - Ch^{1/2}$ for the case of $\gamma_p = \gamma_f = \gamma$.

THEOREM 4.7. *If $\gamma_p = \gamma_f = \gamma$, then*

$$\begin{aligned} a_p(e_{\phi,h}^k, e_{\phi,h}^k) + a_f(e_{u,h}^k, e_{u,h}^k) + \|e_{p,h}^k\|_{L^2(\Omega_f)}^2 + \|\epsilon_{p,h}^k\|_{\Gamma}^2 + \|\epsilon_{f,h}^k\|_{\Gamma}^2 \\ \leq C(1 - C\gamma(\|\mathbb{K}^{-1}\|^{1/2} + \gamma h^{-1/2}\|\mathbb{K}\|^{1/2})^{-2})^{\lfloor \frac{k}{2} \rfloor} (\|\epsilon_p^0\|_{\Gamma}^2 + \|\epsilon_f^0\|_{\Gamma}^2). \quad \blacksquare \end{aligned}$$

REMARK 4.8. One important question is how to choose the parameter γ so that the Robin-Robin domain decomposition method has fast/optimal convergence rate. The analysis above suggests that the optimal choice of the parameter may depend on both the mesh grid size h and the hydraulic conductivity tensor \mathbb{K} .

One possible choice of γ is to balance the terms $\gamma^{-1}\|\mathbb{K}^{-1}\|$ and $\gamma h^{-1}\|\mathbb{K}\|$ and let $\gamma = \frac{\|\mathbb{K}^{-1}\|^{1/2} h^{1/2}}{\|\mathbb{K}\|^{1/2}}$. Then,

$$\frac{\gamma}{(\|\mathbb{K}^{-1}\|^{1/2} + \gamma h^{-1/2}\|\mathbb{K}\|^{1/2})^2} = \frac{h^{1/2}}{\|\mathbb{K}^{-1}\|^{1/2}\|\mathbb{K}\|^{1/2}}. \quad (4.9)$$

Now, if we assume that $\mathbb{K} = K\mathbb{I}$, then $\|\mathbb{K}^{-1}\|^{1/2}\|\mathbb{K}\|^{1/2} = 1$, so the convergence rate of the Robin-Robin domain decomposition finite element method is $1 - Ch^{1/2}$.

In the case $\gamma_f \neq \gamma_p$, we have the same result as Theorem 3.4 with geometric convergence with rate independent of h .

THEOREM 4.9. *If (3.21) is satisfied, then*

$$a_p(e_{\phi,h}^k, e_{\phi,h}^k) + a_f(e_{u,h}^k, e_{u,h}^k) + \|e_{p,h}^k\|_{L^2(\Omega_f)}^2 + \|\epsilon_{p,h}^k\|_{\Gamma}^2 + \|\epsilon_{f,h}^k\|_{\Gamma}^2 \leq C \left(\frac{\gamma_f}{\gamma_p} \right)^k (\|\epsilon_{p,h}^0\|_{\Gamma}^2 + \|\epsilon_{f,h}^0\|_{\Gamma}^2).$$

Now we consider the case $\gamma_f > \gamma_p$ which is counter-intuitive in view of Lemma 3.2. Nevertheless, at the discrete level, we are able to control the excessive growth term by the decay terms so long as the parameters γ_f and γ_p are chosen to be close (depending on \mathbb{K} and h). Indeed, thanks to Lemma 4.4, we have

$$\begin{aligned} & \left(\left(\frac{\gamma_f}{\gamma_p} \right)^2 - 1 \right) \|\epsilon_{p,h}^k\|_{\Gamma}^2 - \gamma_f \left(1 + \frac{\gamma_f}{\gamma_p} \right) g a_p(e_{\phi,h}^k, e_{\phi,h}^k) \\ & \leq \left(\left(\left(\frac{\gamma_f}{\gamma_p} \right)^2 - 1 \right) C (\|\mathbb{K}^{-1}\|^{1/2} + \gamma_p h^{-1/2} \|\mathbb{K}\|^{1/2})^2 - \gamma_f \left(1 + \frac{\gamma_f}{\gamma_p} \right) g \right) a_p(e_{\phi,h}^k, e_{\phi,h}^k) \\ & = \gamma_f \left(1 + \frac{\gamma_f}{\gamma_p} \right) \left(\left(\frac{1}{\gamma_p} - \frac{1}{\gamma_f} \right) C (\|\mathbb{K}^{-1}\|^{1/2} + \gamma_p h^{-1/2} \|\mathbb{K}\|^{1/2})^2 - g \right) a_p(e_{\phi,h}^k, e_{\phi,h}^k) \\ & \leq 0 \end{aligned}$$

provided that the following condition holds

$$0 \leq \frac{1}{\gamma_p} - \frac{1}{\gamma_f} \leq \frac{g}{C(\|\mathbb{K}^{-1}\|^{1/2} + \gamma_p h^{-1/2} \|\mathbb{K}\|^{1/2})^2}. \quad (4.10)$$

An undesirable feature here is the dependence on the mesh size h . For every small h , the γ s must be very close in order to have the above inequality satisfied. This would lead to a very slow convergence rate.

We then have, when combined with Lemma 4.3 and under the assumption (4.10),

$$\begin{aligned} \|\epsilon_{p,h}^{k+1}\|_{\Gamma}^2 &\leq \|\epsilon_{f,h}^k\|_{\Gamma}^2 - 2(\gamma_f + \gamma_p)a_f(\mathbf{e}_{u,h}^k, \mathbf{e}_{u,h}^k) \leq \|\epsilon_{f,h}^k\|_{\Gamma}^2 - 4\gamma_p a_f(\mathbf{e}_{u,h}^k, \mathbf{e}_{u,h}^k) \\ \|\epsilon_{f,h}^{k+1}\|_{\Gamma}^2 &\leq \|\epsilon_{p,h}^k\|_{\Gamma}^2 - \gamma_f \left(1 + \frac{\gamma_f}{\gamma_p}\right) g a_p(e_{\phi,h}^k, e_{\phi,h}^k) \leq \|\epsilon_{p,h}^k\|_{\Gamma}^2 - 2\gamma_f g a_p(e_{\phi,h}^k, e_{\phi,h}^k). \end{aligned}$$

Summing the two inequalities for k from 0 to N , we deduce the convergence of $e_{\phi,h}^k$ and $\mathbf{e}_{u,h}^k$ that leads to the convergence (without rate) of all quantities involved. A rate of convergence can be derived just as in the case of $\gamma_p = \gamma_f$. Indeed, we may deduce, with the help of Lemma 4.4 and the last inequality above,

$$\|\epsilon_{f,h}^{k+1}\|_{\Gamma}^2 \leq (1 - C\gamma_f(\|\mathbb{K}^{-1}\|^{1/2} + \gamma_p h^{-1/2}\|\mathbb{K}\|^{1/2})^{-2})\|\epsilon_{p,h}^k\|_{\Gamma}^2$$

and hence we obtain

$$\begin{aligned} \|\epsilon_{p,h}^{k+1}\|_{\Gamma}^2 &\leq (1 - C\gamma_f(\|\mathbb{K}^{-1}\|^{1/2} + \gamma_p h^{-1/2}\|\mathbb{K}\|^{1/2})^{-2})\|\epsilon_{p,h}^{k-1}\|_{\Gamma}^2 \\ \|\epsilon_{f,h}^{k+1}\|_{\Gamma}^2 &\leq (1 - C\gamma_f(\|\mathbb{K}^{-1}\|^{1/2} + \gamma_p h^{-1/2}\|\mathbb{K}\|^{1/2})^{-2})\|\epsilon_{f,h}^{k-1}\|_{\Gamma}^2. \end{aligned}$$

This further implies convergence with convergence rate proportional to $1 - Ch^{1/2}$ for the case of $\gamma_p < \gamma_f$ under the additional constraint of (4.10). Therefore, we have proved the following theorem.

THEOREM 4.10. *For $\gamma_p < \gamma_f$, assume that the additional constraint (4.10) holds. Then, we have the following convergence result for our parallel Robin-Robin domain decomposition finite element methods for the coupled Stokes-Darcy system:*

$$\begin{aligned} a_p(e_{\phi,h}^k, e_{\phi,h}^k) + a_f(\mathbf{e}_{u,h}^k, \mathbf{e}_{u,h}^k) + \|e_{p,h}^k\|_{L^2(\Omega_f)}^2 + \|\epsilon_{p,h}^k\|_{\Gamma}^2 + \|\epsilon_{f,h}^k\|_{\Gamma}^2 \\ \leq C(1 - C\gamma_f(\|\mathbb{K}^{-1}\|^{1/2} + \gamma_p h^{-1/2}\|\mathbb{K}\|^{1/2})^{-2})^{\lfloor \frac{k}{2} \rfloor} (\|\epsilon_p^0\|_{\Gamma}^2 + \|\epsilon_f^0\|_{\Gamma}^2). \end{aligned}$$

5. Computational experiments. We present some preliminary computational results based on the parallel Robin-Robin domain decomposition finite element method for the coupled Stokes-Darcy system with Beavers-Joseph-Saffman-Jones interface boundary condition. In order to make direct comparisons with [8], we also present computational results for the simplified boundary condition

$$\boldsymbol{\tau}_j \cdot \mathbf{u}_f = 0$$

used in that paper instead of the Beavers-Joseph-Saffman-Jones interface boundary condition (1.2). This simplified interface boundary condition can be formally derived in the limit of $\alpha \rightarrow \infty$ in (1.2).

We consider two test problems. The first is the example from [8].

Example 1: Let $\Omega_p = (0, 1) \times (0, 1)$, $\Omega_f = (0, 1) \times (1, 2)$, and $\Gamma = \{0 \leq x \leq 1, y = 1\}$. The exact solution is given by

$$\begin{aligned} (\mathbf{u}_f)_1 &= y^2 - 2y + 1 \quad (\mathbf{u}_f)_2 = x^2 - x \\ p &= 2\nu(x + y - 1) + 1/(3K) \quad \phi = (x(x-1)(y-1) + \frac{y^3}{3} - y^2 + y)/K + 2x\nu. \end{aligned}$$

The data in the Stokes-Darcy problem is manufactured using this exact solution.

The second test problem is physically more realistic.

Example 2: Let $\Omega_p = (0, \pi) \times (-1, 0)$, $\Omega_f = (0, \pi) \times (0, 1)$, and $\Gamma = \{0 \leq x \leq \pi, y = 0\}$. Let $v(y)$ denote any function that satisfies the boundary conditions $v(0) = -2K$ and $v'(\pi) = 0$ and let

$$u_{f,1} = v'(y) \cos x \quad u_{f,2} = v(y) \sin x \quad p_f = 0 \quad \phi_p = (e^y - e^{-y}) \sin x.$$

Assume that the hydraulic conductivity is homogeneous and isotropic, i.e., $\mathbb{K} = K\mathbb{I}$. Then, for any $v(y)$ satisfying the boundary conditions $v(0) = -2K$ and $v'(\pi) = 0$, these functions exactly satisfy the Stokes-Darcy system with the simplified interface condition (5) (but with inhomogeneous Dirichlet boundary condition on $\partial\Omega$). For example, we may take $v(y) = -2K + c \sin^2(\pi y)$. If $c = \frac{K}{\pi^2}$, then these functions also satisfy the Beavers-Joseph-Saffman-Jones interface boundary condition with any α . The data in the Stokes-Darcy problem is manufactured using these function as the exact solution.

REMARK 5.1. More complex versions of Example 2 can be easily constructed. For instance, a nontrivial pressure field can be considered by simply making sure that $p_f(x, 0) = 0$ and then update the body force \mathbf{f} accordingly. We may even construct an exact solution for which the homogeneous boundary condition for the hydraulic head ϕ_p is satisfied at the expense of introducing an additional (artificial) body force for the Darcy system. Additional examples satisfying the Beavers-Joseph-Saffman-Jones interface boundary condition (1.2) instead of the simplified interface boundary condition (5) can be derived easily as well. One merely needs to arrange for $v(0) = -2K$, $v'(\pi) = 0$, and $v''(\pi) = 2K$ as in example 2. Alternatively, we could set $v(y) = -2K + Ky^2 + cy^3$ in example 2. For domains with flat boundaries, we may also use symbolic computational tools to find exact solutions (even with Beavers-Joseph-Saffman-Jones interface boundary condition) that are quadratic in the velocity, linear in the pressure, and cubic in the hydraulic head. Example 1 is a special case.

5.1. Convergence of the finite element method. Here we address the issue of the convergence of the finite element method, i.e., we directly solve the full coupled Stokes-Darcy system without using domain decomposition. Recall that we use P_2 elements to approximate ϕ_p on the domain Ω_p and the Hood-Taylor element pair $((P_2)^2$ for \mathbf{u}_f and P_1 for p_f) on the domain Ω_f . We use a uniform triangular meshes constructed by subdividing the rectangular domain Ω into squares of side h and then dividing each square into two triangles. We compute the finite element approximation using the sequence of grid sizes $h = 2^{-m}$, $m = 1, \dots, 6$. Errors are measured using the discrete ℓ^2 norm which is proportional to the $L^2(\Omega_f)$ error, modulo a factor of h^2 . We presume that the relative error in the approximation to the velocity in the fluid satisfies

$$\text{relative error} = \frac{\|\mathbf{u}_f - \mathbf{u}_{f,m}\|}{\|\mathbf{u}_f\|} \approx Ch^\alpha = C \left(\frac{1}{2^m} \right)^\alpha$$

for some α , where $\mathbf{u}_{f,m}$ denotes the finite element approximation obtained with $h = 2^{-m}$. Then, we have that

$$\log(\text{relative error}) = \log \frac{\|\mathbf{u}_f - \mathbf{u}_{f,m}\|}{\|\mathbf{u}_f\|} \approx \log C - m\alpha \log 2$$

and

$$\text{convergence factor} = \frac{\|\mathbf{u}_f - \mathbf{u}_{f,m}\|}{\|\mathbf{u}_f - \mathbf{u}_{f,m+1}\|} = 2^\alpha.$$

In Figures 5.1 and 5.3, the log of the relative error and the convergence factor are plotted versus m . Similar plots are given for ϕ_p in Figures 5.2 and 5.4. Since we are using quadratic finite element spaces for both ϕ_p and \mathbf{u}_f , we expect that $\alpha = 3$ so that we expect a convergence factor of 8 and a slope in the relative error curve equal to $3 \log 2$.

There are two noteworthy observations that may be gleaned from the computational results.

- The convergence rates depend on the parameters \mathbb{K} and ν .
- For the case $\mathbb{K} = K\mathbb{I}$ and $\nu = 1$, it seems that we have super-convergence, i.e.,

$$\frac{\|\mathbf{u}_f - \mathbf{u}_{f,h}\|}{\|\mathbf{u}_{f,h}\|} \approx \mathcal{O}(h^{3.5}) \quad \frac{\|\phi_p - \phi_{p,h}\|}{\|\phi_{p,h}\|} \approx \mathcal{O}(h^{3.5}).$$

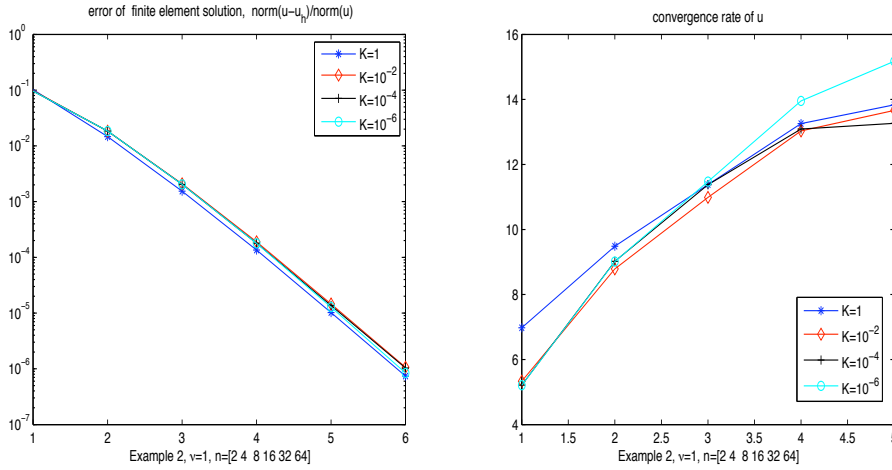


FIG. 5.1. Relative error (left) and convergence factor (right) of the finite element approximation of \mathbf{u}_f versus m for Example 2 with $\nu = 1$.

5.2. Convergence of the Robin-Robin domain decomposition method.

We now consider the differences between iterations of the Robin-Robin domain decomposition method and the exact solution of the discrete finite element problems. Specifically, in the figures that follow, we plot the ℓ^2 norm of $(\mathbf{u}_{f,h}^k - \mathbf{u}_{f,h})$ versus the iteration counter k . The computational results presented confirm our theoretical convergence analysis.

By setting $K = 1$, $\nu = 1$ and $\gamma_f = 1$, Figure 5.5 shows that, for the parallel Robin-Robin domain decomposition method,

- if $\gamma_f < \gamma_p$ ($\gamma_p = \frac{1}{3}\gamma_f$ or $\frac{1}{2}\gamma_f$), convergence is very fast; the error is reduced by a factor of γ_f/γ_p every two steps;
- if $\gamma_f > \gamma_p$ ($\gamma_p = 3\gamma_f$ or $2\gamma_f$), the iterative method diverges;
- if $\gamma_f = \gamma_p$, the iterative method converges, but with a slow rate.

It is interesting to compare the parallel and serial versions of the Robin-Robin domain decomposition method. Note that the serial version of our algorithm is just the sRR algorithm of [8]. Figure 5.6 shows the results for the serial version. Comparing with Figure 5.5, we see that the behaviors of the two methods are similar except that

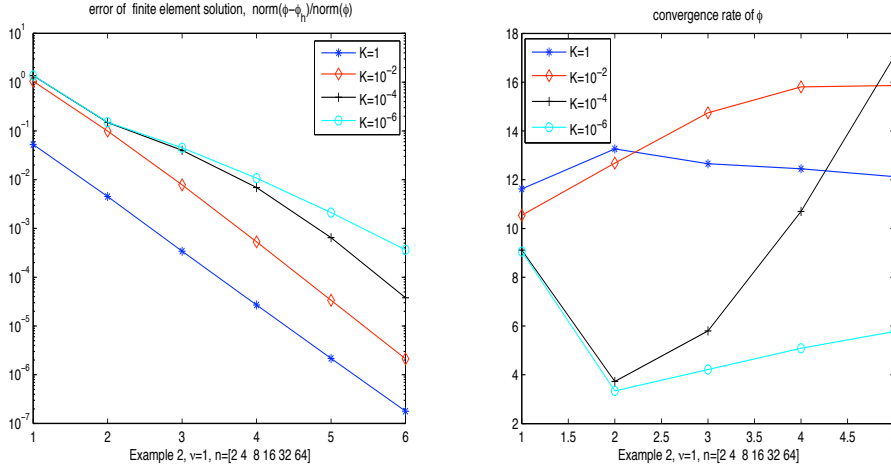


FIG. 5.2. Relative error (left) and convergence factor (right) of the finite element approximation of ϕ_p versus m for Example 2 with $\nu = 1$.

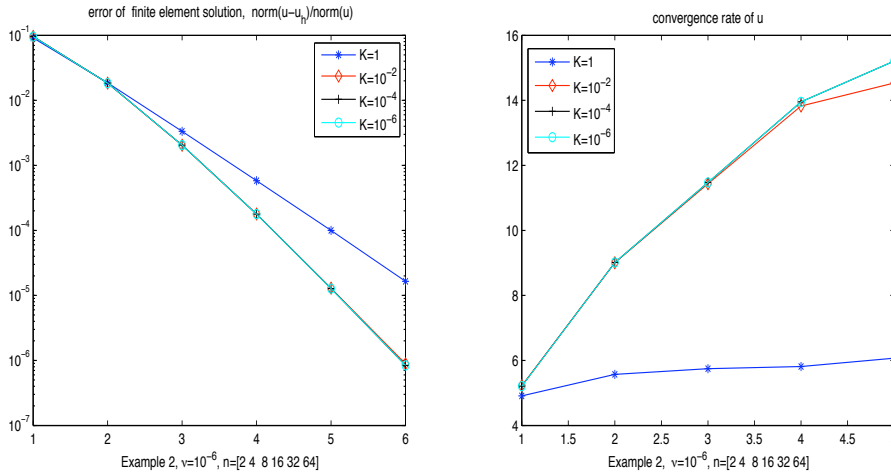


FIG. 5.3. Relative error (left) and convergence factor (right) of the finite element approximation of u_f versus m for Example 2 with $\nu = 10^{-6}$.

the error for the serial version reduces or increases about two times faster, as the case may be, than the error for the parallel version.

5.3. Possible choice of γ . In (4.9), we point that γ can be chosen as $\gamma = \sqrt{h}/K$ which leads to same convergence rate for different $\mathbb{K} = K\mathbb{I}$. We set the parameters $\nu = 1, K = 1, 10^{-2}, 10^{-4}, 10^{-6}, 10^2, 10^4, 10^6$.

Figure 5.7 shows that the convergence rates are similar; for large K , the convergence rates are same. Note that the exact solution depends on the parameters ν and K , therefore the errors of the initial step are different, so it is better to compare the decreased speed of the error.

5.4. The choice of the parameters γ_f and γ_p . It is interesting to point out that our scheme converges in the case of $\gamma_f \leq \gamma_p$ which is contrary to [8]. In fact,

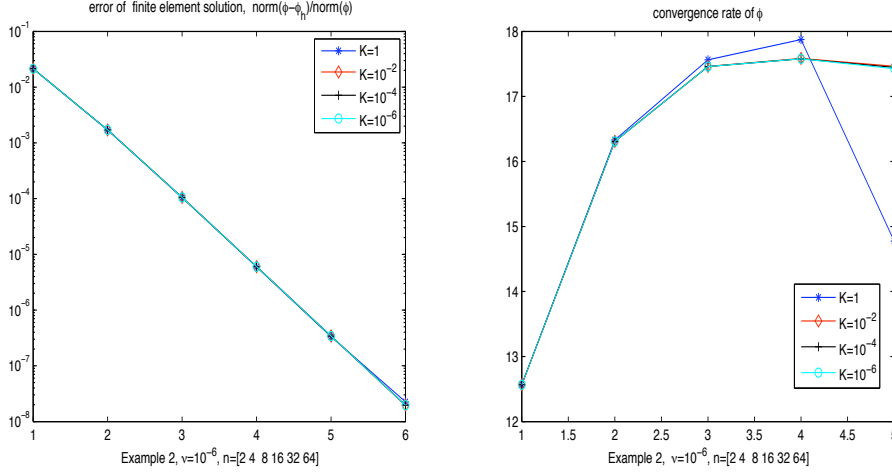


FIG. 5.4. Relative error (left) and convergence factor (right) of the finite element approximation of ϕ_p versus m for Example 2 with $\nu = 10^{-6}$.

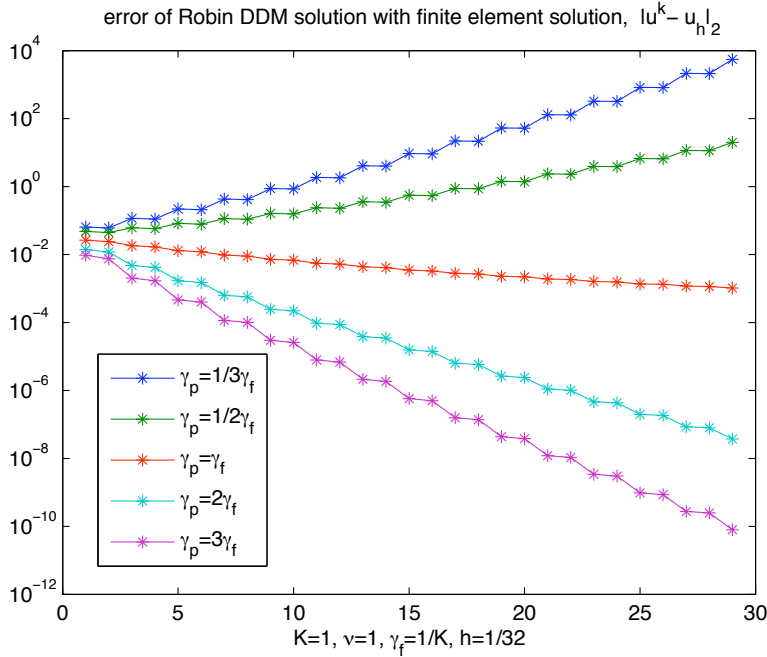


FIG. 5.5. Error in the iterates versus the iteration counter k for the parallel Robin-Robin domain decomposition method.

for their choice of acceleration parameters $\gamma_f = 0.3, \gamma_p = 0.1$, we observe numerical instability of the iterative process.

The parameters γ_f and γ_p should be chosen carefully. Let us repeat the numerical experiments in [8], where the sRR algorithm (i.e. the serial version of our Robin-Robin algorithm) shows very attractive results for $\gamma_f = 0.3, \gamma_p = 0.1$. However, the results

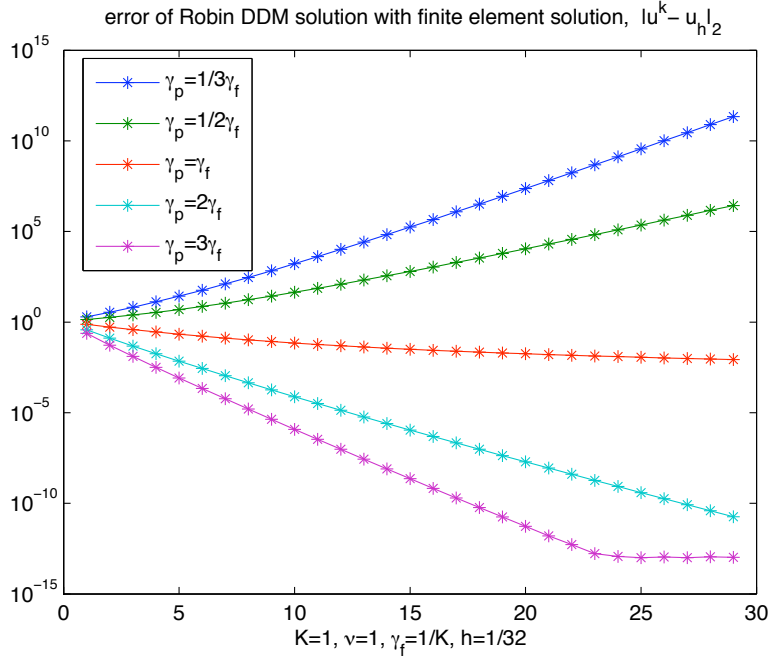


FIG. 5.6. Error in the iterates versus the iteration counter k for the serial Robin-Robin domain decomposition method.

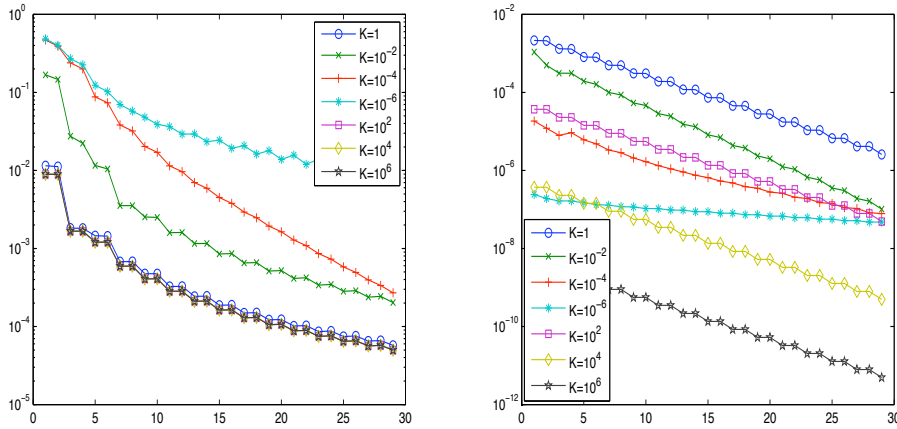


FIG. 5.7. $\gamma_f = \gamma_p = \sqrt{h}/K$. Left figure is for Example 1 and right figure is for Example 2.

seems to be re-analyze carefully.

In our numerical experiment we set $\gamma_p = 0.1$ and $\gamma_f = 1/3\gamma_p, 1/2\gamma_p, \gamma_p, 2\gamma_p, 3\gamma_p$, our numerical results show that the convergence behavior is complicated (See Fig.5.8 and Fig.5.9). Especially, when $\gamma_p = 0.1$ and $\gamma_f = 3\gamma_p = 0.3$, for $\mathbb{K} = \mathbb{I}$ and $\nu = 1$, the serial DDM method diverges!

Comparing with the parallel Robin-Robin DDM method (see Fig. 5.10 and Fig.

5.11), we can conclude that both two methods have same convergence behavior.

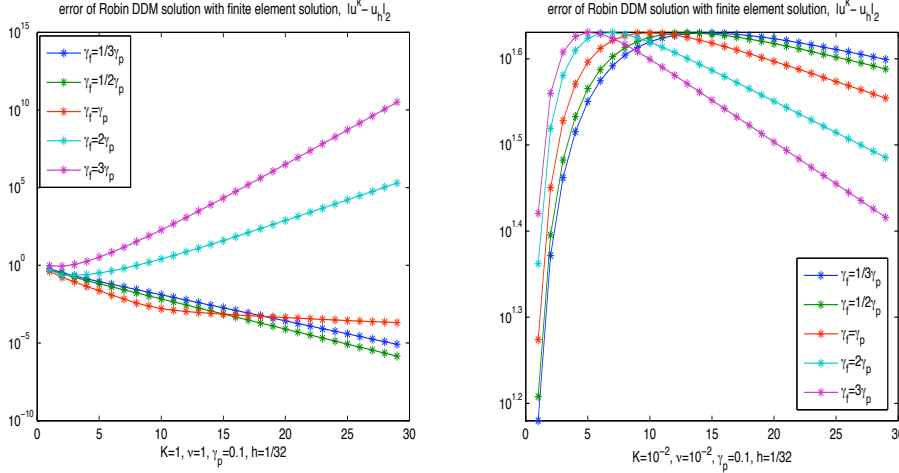


FIG. 5.8. Serial Robin-Robin DDM. Left: $K = \nu = 1$; right: $K = \nu = 10^{-2}$.

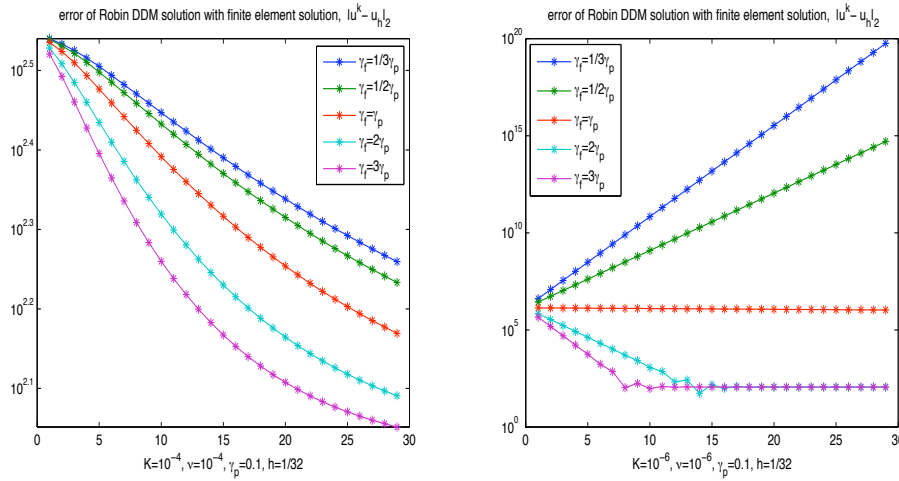


FIG. 5.9. Serial Robin-Robin DDM. Left: $K = \nu = 10^{-4}$; right: $K = \nu = 10^{-6}$.

5.5. Iteration numbers and meshsize. According to our theoretic results, for the case of $\gamma_f \neq \gamma_p$, the numbers of Robin-Robin DDM iterations is independent of the grid size if the DDM method is convergent, and for the case of $\gamma_f = \gamma_p$, the numbers of Robin-Robin DDM iterations is slight dependent of the grid size. Now we set $n = 2, 4, 8, 16, 32$ and the mesh size is $h = \frac{1}{n}$. We terminate the iteration process if the relative increment of the trace of the discrete normal velocity on the interface $\mathbf{u}_{f,h}^k \cdot \mathbf{n}|_\Gamma$ is less than the tolerance 10^{-6} . We also terminate iteration process if the iteration number is bigger than maximum iterative steps 400, which is denoted by the sign ‘-’ in the table 5.1. The results in table 5.1 confirm our theoretic estimates.

REFERENCES

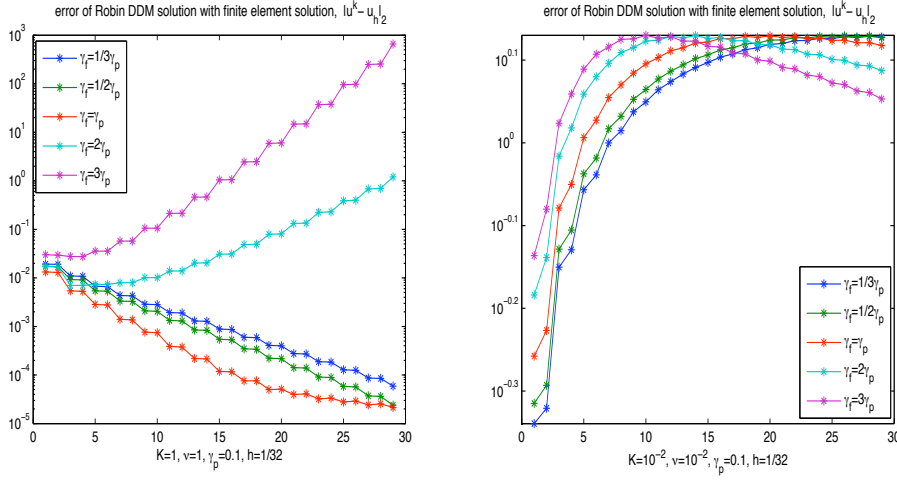


FIG. 5.10. *Parallel Robin-Robin DDM. Left: $K = \nu = 1$; right: $K = \nu = 10^{-2}$.*

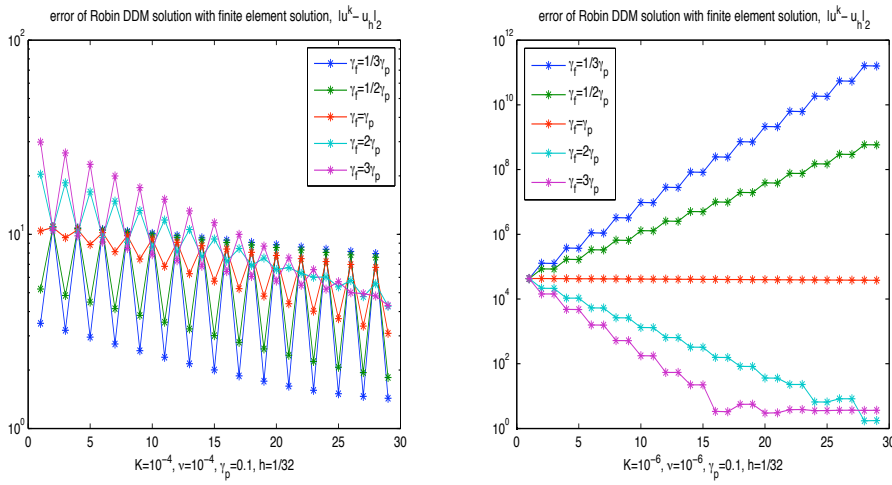


FIG. 5.11. *Parallel Robin-Robin DDM. Left: $K = \nu = 10^{-4}$; right: $K = \nu = 10^{-6}$.*

n	$\gamma_p = 0.1, \gamma_f = \frac{\gamma_p}{3}$				$\gamma_p = 0.1, \gamma_f = \gamma_p$		
	(1, 1)	(1, 10^{-2})	(10^2 , 1)	(10^2 , 10^{-2})	(1, 1)	(1, 10^{-2})	(10^2 , 10^{-2})
2	44	60	14	18	28	36	337
4	42	56	14	18	52	42	339
8	42	54	14	18	80	70	349
16	42	54	14	18	114	110	367
32	42	54	14	18	140	164	-

TABLE 5.1

The numbers of iterations. Here (a, b) means $K = a, \nu = b$.

- [1] G. BEAVERS AND D. JOSEPH, *Boundary conditions at a naturally permeable wall*, J. Fluid Mech., 30(1967), pp. 197-207.
- [2] Y. CAO, M. GUNZBURGER, F. HUA AND X. WANG, *Coupled Stokes-Darcy Model with Beavers-Joseph Interface Boundary Condition*, Comm. Math. Sci., to appear.
- [3] P. CIARLET, *The Finite Element Method for Elliptic Problems*, Amsterdam, North-Holland,

- 1978.
- [4] Q. DENG, *An analysis for nonoverlapping domain decomposition iterative procedure*, SIAM J. Sci. Comput., 18(1997), pp. 1517-1525.
 - [5] Q. DENG, *A nonoverlapping domain decomposition method for nonconforming finite element problems*, Commun. Pure Appl. Anal., 2(2003), pp. 295-306.
 - [6] M. DISCACCIATI, E. MIGLIO AND A. QUARTERONI, *Mathematical and numerical models for coupling surface and groundwater flows*, Appl. Num. Math., 43(2002), pp. 57-74.
 - [7] M. DISCACCIATI AND A. QUARTERONI, *Convergence analysis of a subdomain iterative method for the finite element approximation of the coupling of Stokes and Darcy equations*, Comput. Vis. Sci., 6(2004), pp. 93-103.
 - [8] M. DISCACCIATI, A. QUARTERONI AND A. VALLI, *Robin-Robin domain decomposition methods for the Stokes-Darcy coupling*, SIAM J. Numer. Anal., 45(2007), pp. 1246-1268.
 - [9] M.-J. GANDER, L. HALPERN, AND F. NATAF, *Optimized Schwarz methods*, in Twelfth International Conference on Domain Decomposition methods, Chiba, Japan, 2001, pp. 15-28.
 - [10] V. GIRAULT AND P.-A. RAVIART, *Finite Element Methods for Navier-Stokes Equations*, Springer-Verlag, Berlin 1986.
 - [11] M. GUNZBURGER, *Finite Element Methods for Viscous Incompressible Flows: A Guide to Theory, Practice, and Algorithms*, Academic Press, Boston 1989.
 - [12] I. JONES, *Low Reynolds number flow past a porous spherical shell*, Proc. Camb. Phil. Soc., 73(1973), pp. 231-238.
 - [13] P.-L. LIONS, *On the Schwarz alternating method III: a variant for nonoverlapping subdomains*, in Third International Symposium on Domain Decomposition Methods for PDEs, T.F. Chan, R. Glowinski, J. Périaux, and O.B. Widlund, eds., SIAM, Philadelphia, 1990, pp. 202-231.
 - [14] M. MU AND J. XU, *A two-grid method of a mixed Stokes-Darcy model for coupling fluid flow with porous media flow*, SIAM J. Numer. Anal., 45(2007), pp. 1801-1813.
 - [15] A. QUARTERONI AND A. VALLI, *Domain Decomposition Methods for Partial Differential Equations*, Oxford Science Publications, Oxford, 1999.
 - [16] L. QIN, Z.-C. SHI AND X. XU, *On the convergence rate of a parallel nonoverlapping domain decomposition method*, Sci. China, Ser. A.: Mathematics, 51(2008), pp. 1461 - 1478.
 - [17] L. QIN AND X. XU, *On a parallel robin-type nonoverlapping domain decomposition method*, SIAM J. Numer. Anal., 44(2006), pp. 2539-3558.
 - [18] L. QIN AND X. XU, *Optimized schwarz methods with robin transmission conditions for parabolic problems*, SIAM J. Sci. Comput., 31(2008), pp. 608-623.
 - [19] P. SAFFMAN, *On the boundary condition at the interface of a porous medium*, Stud. in Appl. Math., 1(1971), pp. 77-84.
 - [20] B. SMITH, P. BJØRSTAD AND W. GROPP, *Domain Decomposition: Parallel Multilevel Methods for Elliptic Partial Differential Equations*, Cambridge University Press, 1996.
 - [21] A. TOSELLI AND O. WIDLUND, *Domain Decomposition Methods – Algorithms and Theory*, Springer-Verlag, 2005.